ACS Catalysis

pubs.acs.org/acscatalysis

Research Article

Origins of Regio- and Chemoselectivity in Iron-PDAI-Catalyzed [2+2+2] Cycloaddition Syntheses of 4,6-Disubstituted 2-Aminopyridines

Jordan L. Harper,[§] Stephanie Felten,[§] Ryan M. Stolley, Alexander S. Hegg, Paul H.-Y. Cheong,* and Janis Louie*

Cite This: *ACS Catal.* 2021, 11, 14677−14687

Read Online

ACCESS | Metrics & More | Article Recommendations | Supporting Information

ABSTRACT: A mechanistic investigation into the origins of the regio- and chemoselectivities observed in iron/pyridine dialdimine (PDAI)-catalyzed intermolecular [2+2+2] cycloaddition reactions of terminal alkynes and cyanamides to yield substituted 2-aminopyridines is reported. The combination of experimental and computational studies disclosed herein reveals the role of the hemilabile PDAI ligand as an important factor controlling the resultant product's observed regio- and chemoselectivity.

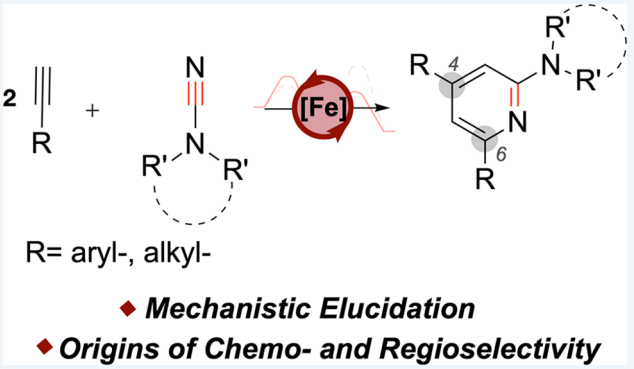

KEYWORDS: *heterocycles, catalysis, 2-aminopyridines, cycloaddition, mechanism, iron*

INTRODUCTION

Metal-catalyzed [2+2+2] cycloaddition reactions are a valuable tool in synthetic organic chemistry that allow access to substituted carbo- and heterocycles in a one-step reaction. The high atom and step economy and the broad functional group tolerance of such reactions are highly appealing for synthetic chemists.[1−8] Literature reports illustrate myriad efficient catalytic species (e.g., Rh,[9−15] Ru,[16−24] Ir,[25−29] Co,[30−40] Ni,[41−47] Nb,[48] Au,[49] Cu,[50] Fe[51−59]) and coupling partners (e.g., olefins, nitriles, isocyanates, cyanamides, aldehydes, ketones, carbon dioxide, imines, carbodiimides), which highlight the great potential of these cycloaddition reactions.[1−8] Furthermore, their broad applicability is demonstrated by the diversity of synthetic strategies that incorporate these reactions as a key step in the synthesis of natural products,[60−65] polymers,[66,67] electroluminescent materials,[68−70] and other aromatic building blocks[2,3,5,6] (Scheme 1, **A**).

Despite allowing access to highly functionalized cyclic products, lack of control over chemo- and regioselectivity is a continuing challenge,[1,2,5−8] and it can adversely affect the synthetic utility of these cycloadditions. For instance, the incorporation of triple-bonded π-systems containing hetero atoms is difficult to achieve due to the competing cyclotrimerization of alkynes, which restricts the selective synthesis of a given heterocycle. Furthermore, the selective derivatization to multisubstituted products represents another challenge, and complicated product mixtures of chemo- and regioisomers can be problematic to separate (Scheme 1, **B**).

The development of partially intramolecular [2+2+2] cycloadditions using tethered α,ω-diynes as starting materials has addressed these limitations somewhat, but their overall synthetic utility is nonetheless still limited.[1,2,5−8] For example, though a broad range of valuable compounds can be obtained in partially intramolecular [2+2+2] cycloadditions, the irremovable tethers of the α,ω-diynes are a significant disadvantage in terms of the general utility of the products (Scheme 1, **C**). Although this can be somewhat remedied by synthetic protocols applying removable silyl ether tethers, they are nonetheless still restricted to a narrow substrate scope.[33,71−73]

Though sparse, select examples of regio- and chemoselective analogues of these reactions do exist. The Louie laboratory has developed atom and step economical Ni- and Fe-catalyzed intermolecular [2+2+2] cycloaddition reactions of alkynes and cyanamides that generate 3,5- and 4,6-disubstituted 2-aminopyridines, respectively, in moderate to high yields.[42,57] These

Received: August 25, 2021
Revised: November 4, 2021
Published: November 22, 2021

https://doi.org/10.1021/acscatal.1c03871
ACS Catal. 2021, 11, 14677−14687

Scheme 1. Utility, Demand, and Selectivity Challenges in Metal-Catalyzed Intermolecular [2+2+2] Cycloaddition Syntheses of Heterocyclic Building Blocks

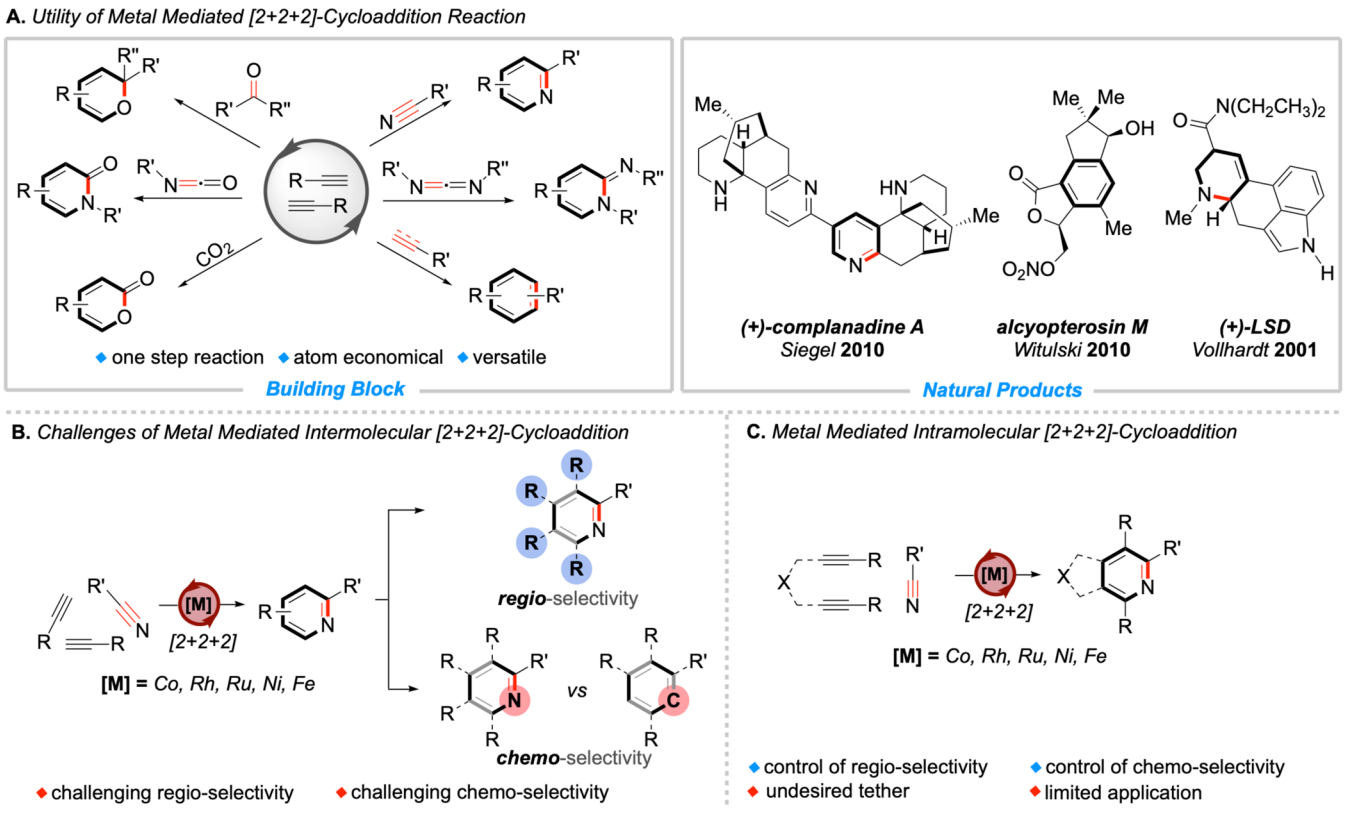

Scheme 2. Overview of Regio- and Chemoselective Nickel-and Iron-Catalyzed Intermolecular [2+2+2] Cycloaddition Syntheses of Disubstituted 2-Aminopyridines

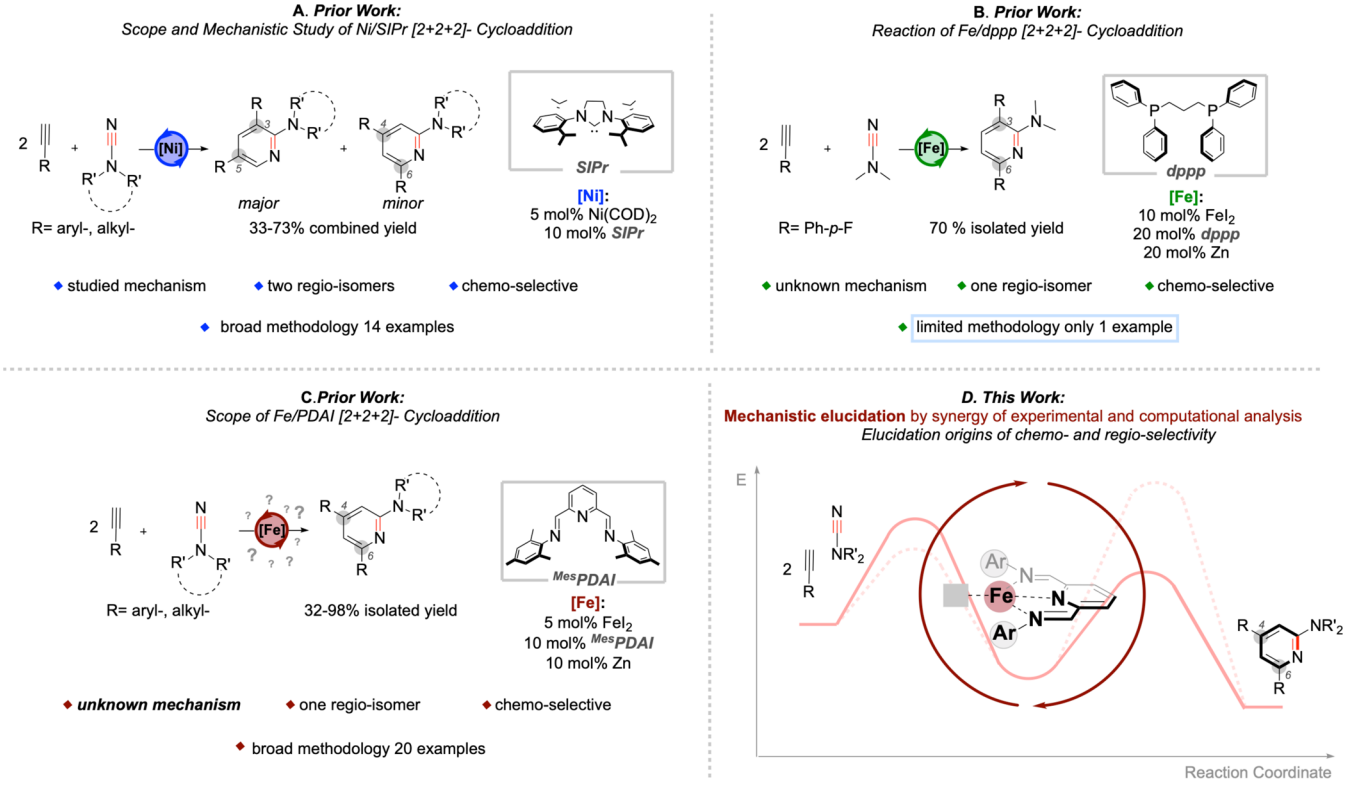

protocols not only utilize mild reaction conditions but also demonstrate high regio- and chemoselectivity depending on the metal-ligand system used. For example, the *in situ* generated Ni/NHC catalyst yielded 3,5- and 4,6- disubstituted 2-amino-

https://doi.org/10.1021/acscatal.1c03871
ACS Catal. 2021, 11, 14677−14687

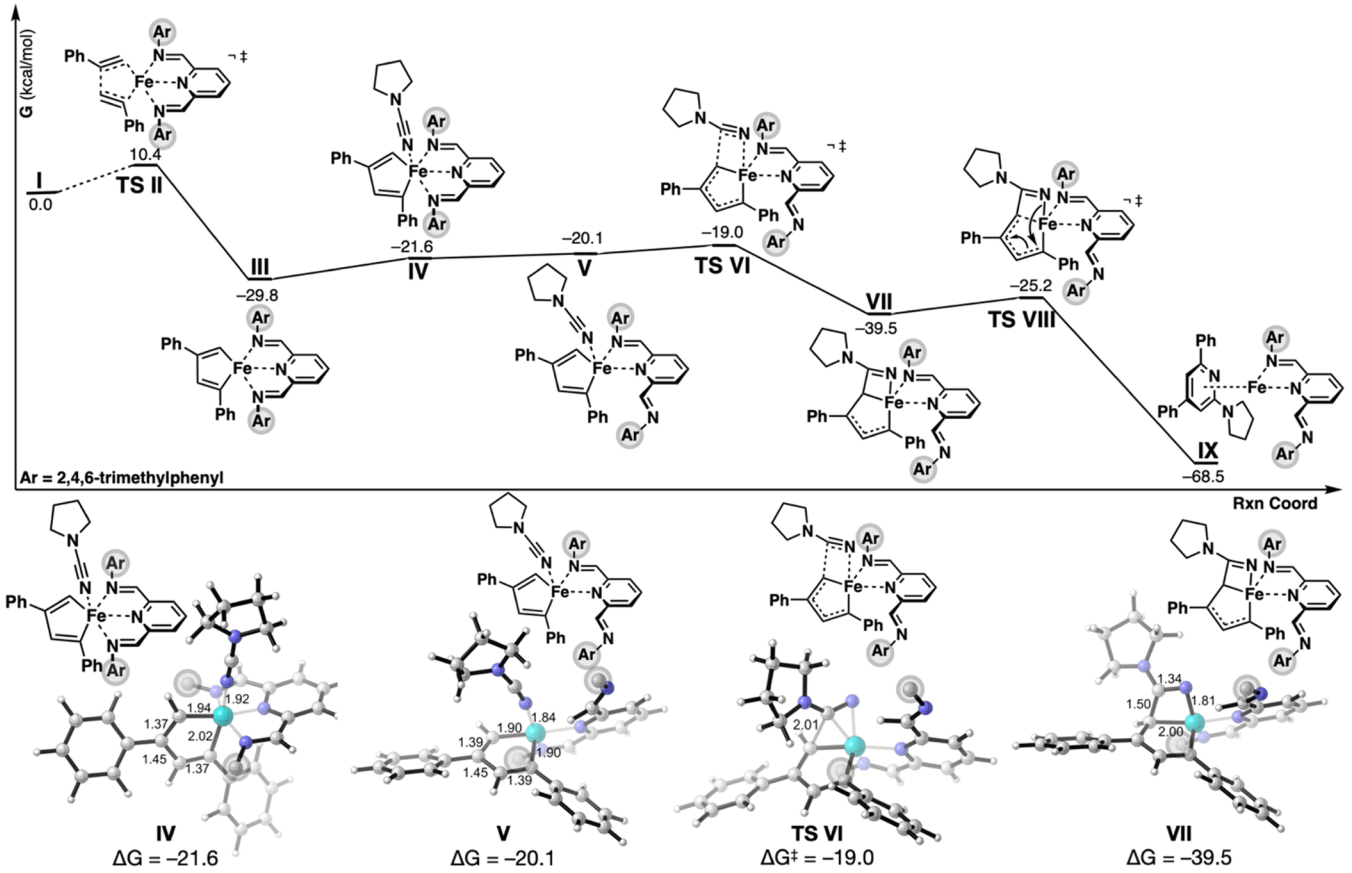

Figure 1. Reaction coordinate diagram of Fe-PDAI [2+2+2] cycloaddition reaction and key major structures. Energies given in kcal/mol; bond lengths given in Å; and catalyst mesityl rings have been rendered invisible for clarity.

pyridine regioisomers with sufficient regiocontrol (14 examples, 33−72% combined yield, Scheme 2, **A**),[42] whereas the *in situ* generated Fe/pyridine dialdimine (PDAI) catalyst selectively formed the 4,6- disubstituted 2-aminopyridine in moderate to excellent yields (20 examples, 32−98% isolated yield, Scheme 2, **C**).[57] The latter synthetic protocol is, to the best of our knowledge, the only method reported in the literature yielding regio- and chemoselective 4,6-disubstituted 2-aminopyridine products via intermolecular [2+2+2] cycloaddition reactions. In a complementary method, Wan and co-workers reported a similar synthetic protocol utilizing an *in situ* generated Fe/phosphine catalyst with which they were able to access a 3,6-disubstituted 2-aminopyridine product selectively; however, their protocol is restricted to a single example (Scheme 2, **B**).[59]

Since divergent selectivity is observed for the Louie and Wan Fe-systems, precedence exists for ligand-controlled regioselectivity. Though ligand-controlled product selectivity is well known in many catalytic processes, the influence of ligands on regioselectivity in metal-catalyzed intermolecular [2+2+2] cycloaddition reactions is rare.[6,7,39,74,75] Current data reveals that regioselectivity is largely dictated by the metal and whether or not a hetero π-system, if present, is incorporated in the first or second coupling step of the cycloaddition. For example, Co-catalyzed [2+2+2] cycloaddition reactions favor homo-oxidative coupling of two alkyne units in the first step of the mechanism and insertion of the hetero π-system as the second step, as do Rh and Ru based systems.[1,5−8,18,20,76−84] In contrast, Ni-based catalysts are proposed to prefer the incorporation of the hetero π-system first in a hetero-oxidative coupling step before the insertion of the second alkyne unit.[1,5−8,42,44,45,85]

Given the high efficiency of Fe/PDAI-catalyzed intermolecular [2+2+2] cycloaddition reactions, we hypothesized that elucidation of the reaction mechanism would uncover the origin of the unique product selectivity observed in these reactions and potentially lay the foundation for future increases in selectivity, catalyst development, and substrate breadth. Thus, we herein report a combined experimental and computational study investigating both the mechanism and the origins of the regio- and chemoselectivities observed in the Fe/PDAI-catalyzed intermolecular [2+2+2] cycloaddition synthesis of alkynes and cyanamide to yield 4,6-disubstituted 2-aminopyridines.

RESULTS

All computations were performed at the PBE/6-31G* level of theory[86,87] in the Gaussian 16 software package,[88] using phenylacetylene and *N*-cyanopyrrolidine as model substrates; *N*-cyanopyrrolidine was chosen over *N*,*N*-dimethylcyanamide to reduce the potential of unwanted negative frequencies occurring in computed structures. The Perdew−Burke−Ernzerhof (PBE) method was chosen to reduce computational time, and all structures were computed in the gas phase; see Supporting Information for benchmarking details. The reaction coordinate diagram and several key structures are shown in Figure 1.

Oxidative Coupling. *Homocoupling vs Heterocoupling.* Transition metal-catalyzed [2+2+2] cycloadditions typically begin with the oxidative coupling of two π systems.[8,79,89] We computed all of the regioisomeric transition states to determine the origins of selectivity for this process (Figure 2).

https://doi.org/10.1021/acscatal.1c03871
ACS Catal. 2021, 11, 14677−14687

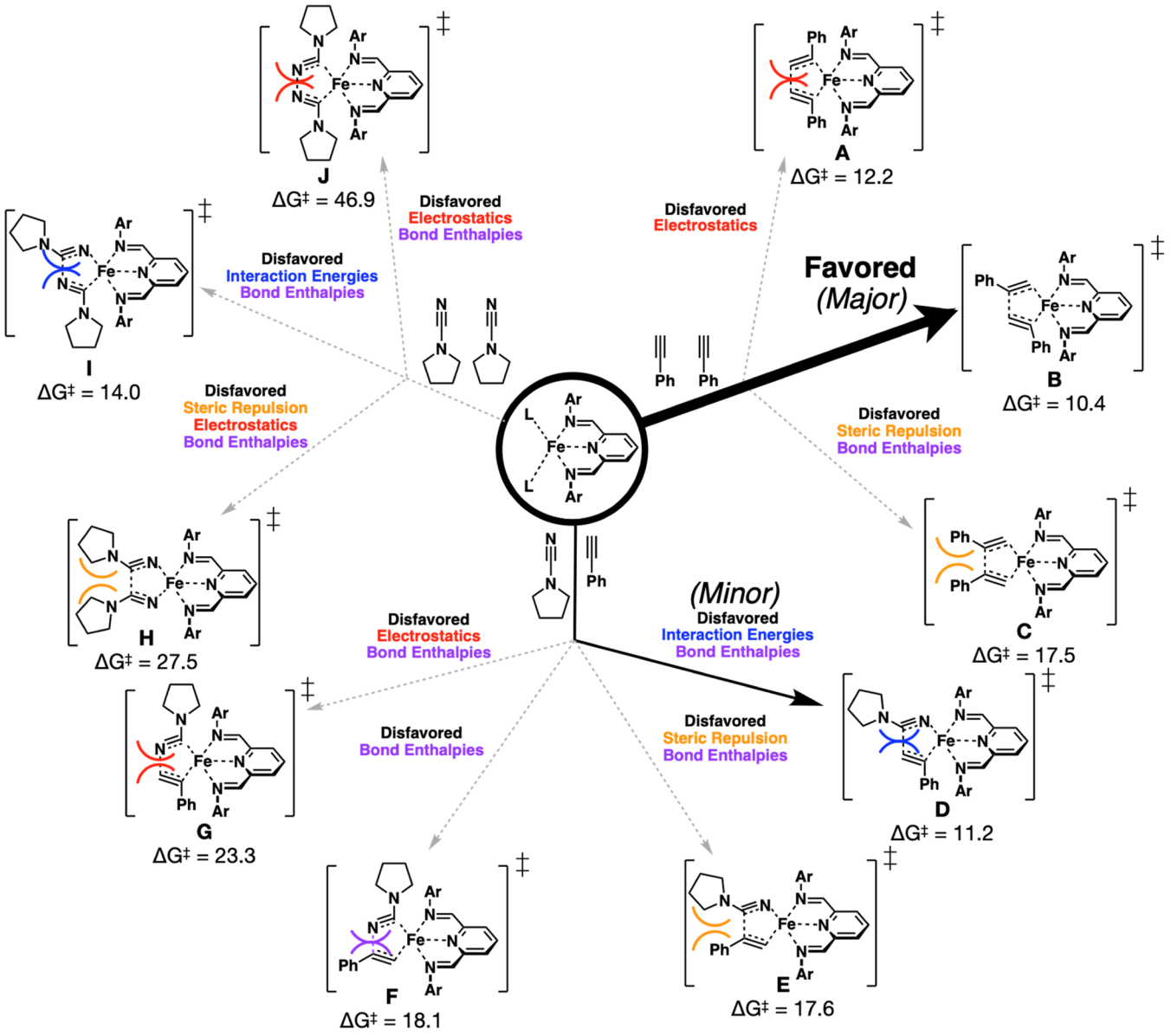

Figure 2. Origins of observed selectivity in oxidative coupling transition states.

Head (substituted end)-to-tail (terminal) bis-alkyne homo-oxidative coupling had a barrier of 10.4 kcal/mol and is the preferred pathway (Figure 2, Structure B). Both isomers of hetero-oxidative coupling between an alkyne and a cyanamide were higher in energy at 11.2 and 18.1 kcal/mol for C−C and C−N bond formation, respectively; homo-oxidative coupling between two cyanamides was also higher in energy, at 14.0 kcal/mol (Figure 2, Structures D, F, and I).

Unsurprisingly, the head-to-head transition states were uniformly disfavored compared to the head-to-tail structures due to steric repulsion between the substituents (Figure 2, Structures C, E, and H). The head-to-head homo-oxidative coupling barriers were 17.5 and 27.5 kcal/mol for the bis-alkyne and bis-cyanamide, respectively, and 17.6 kcal/mol for the alkyne−cyanamide hetero-oxidative coupling.

The tail-to-tail transition states were also disfavored by more than ∼2 kcal/mol, even though these experience minimal steric repulsions. The tail-to-tail homo-oxidative coupling barriers were 12.2 and 46.9 kcal/mol for the bis-alkyne and bis-cyanamide, respectively. The alkyne−cyanamide hetero-oxidative coupling barrier was 23.3 kcal/mol (Figure 2, Structures A, G, and J).

To determine why the tail-to-tail transition states exhibit the above trends, we computed the ChelpG charges of the preceding coordination complexes (Figure 3). Terminal ends of both alkynes and cyanamides bear partial negative charges, while the internal atoms bear partial positive charges. Therefore, unfavorable partial charge interactions are observed in structures

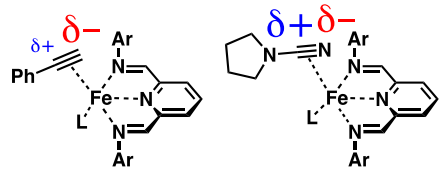

Figure 3. Terminal ends of both alkynes and cyanamides bear partial negative charges, while the internal atoms bear partial positive charges; these charges summarize the electronic effects in the oxidative coupling transition states. Symbol size used to indicate charge magnitude.

https://doi.org/10.1021/acscatal.1c03871
ACS Catal. 2021, 11, 14677−14687

Table 1. Competition Experiment[a]

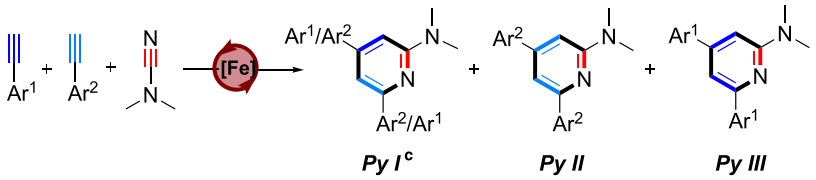

			ratio[b]	yield[b] [%]
entry	Ar^1	Ar^2	Py I: Py II: Py III	Py I: Py II: Py III
1	*p*-Cl	*p*-H	1.00: 0.83: 0.50	35: 29: 17
2	*p*-Cl	*p*-Me	1.00: 0.90: 0.54	36: 32: 19
3	*p*-Cl	*p*-OMe	1.00: 0.75: 0.62	37: 28: 23
4	*p*-F	*p*-H	1.00: 0.39: 0.77	41: 16: 32
5	*p*-F	*p*-Me	1.00: 0.48: 0.80	47: 24: 23
6	*p*-F	*p*-OMe	1.00: 0.27: 0.79	47: 12: 38

[a][Fe]: 5 mol % FeI_2, 10 mol % $^{Mes}PDAI$, 10 mol % Zn, 25 mol % internal standard, tetrahydrofuran (THF) 0.4 M, room-temperature (rt), 24 h, glovebox. [b]Gas chromatography (GC) ratios are based on naphthalene as internal standard. [c]Only one hetero isomer was detected.

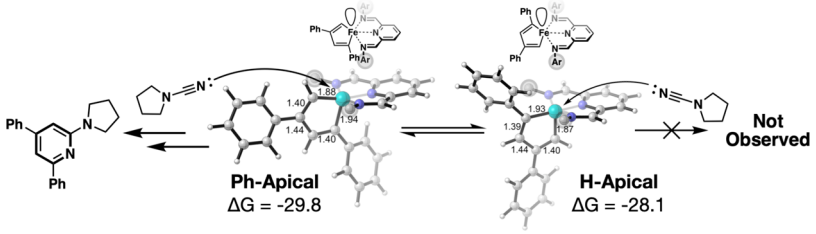

Figure 4. Metallacyclopentadiene reactive intermediates.

where the substituents are in a tail-to-tail or head-to-head orientation. This phenomenon is especially pronounced in the tail-to-tail bis-cyanamide complex, of which the following transition state has an energy barrier of 46.9 kcal/mol (Figure 2, Structure J).

Conversely, the head-to-tail transition states experience favorable partial charge interactions, and interestingly, the head-to-tail alkyne−cyanamide complex exhibits more favorable charge interactions than the bis-alkyne. Despite this, however, unfavorable bond enthalpies, i.e., the conversion of two CC triple bonds vs a CC and a CN triple bond, make bis-alkyne homo-oxidative coupling preferred over alkyne−cyanamide homo-oxidative coupling. In line with this, distortion−interaction analysis also gives a similar conclusion.[90] Less favorable C−N bond enthalpies compared to C−C bond enthalpies also explain why both C−N bond formation in alkyne−cyanamide oxidative heterocoupling is disfavored, as well as bis-cyanamide oxidative homocoupling (see Supporting Information for further discussion).

In general, the homo-oxidative coupling of two alkynes is favored over any analogous hetero-oxidative coupling. Head-to-tail bis-alkyne homo-oxidative coupling is the most preferred overall and is proposed to be the first step of the Fe/PDAI mediated reaction.

Electronic Effects in Homocoupling. In line with the computational results, we find experimentally that electronic perturbations of phenylacetylene do affect the product yield.[57] For example, reactions conducted with the electron-rich 1-ethynyl-4-methoxybenzene afford a higher yield (98%) of 2-aminopyridine product than those utilizing the electron-poor 1-ethynyl-4-fluorobenzene (59%).[57] On the basis of those observations, we were curious about the product distribution in competition experiments between electron-deficient and electron-rich phenylacetylenes in a 1:1:1 reaction stoichiometry with cyanamide, as shown in Table 1. Of the three resultant 2-aminopyridines, the major product is **Py I**, formed by the homo-oxidative coupling of an electron-deficient and an electron-rich alkyne, followed by both **Py II** and **Py III** as minor products from homo-oxidative couplings of two electron-rich and two electron-deficient alkynes, respectively (Table 1, entries 1−3). The reversed yields for the minor products, **Py II** and **Py III**, in the competition experiments conducted with 1-ethynyl-4-fluorobenzene is ostensibly due to the mesomeric (+M) and/or inductive effects of the -F substituent, increasing the reactivity of the 2π alkyne moiety of 1-ethynyl-4-fluorobenzene (Table 1, entries 1−3 versus entries 4−6, respectively). Overall, the experimental observations support the computational analysis and suggest that polarization of the 2π substrates does impact homo-oxidative coupling.

2π Coordination and Ligand Rearrangement. *Cyanamide Coordination.* We next turned our attention to the regioselectivity of the final 2π component incorporation, exploring why only 4,6-diphenyl-2-aminopyridines (**Py I**, Table 1) are observed experimentally and why 3,5-diphenyl-2-aminopyridines are not. A crucial insight into the origin of this regioselectivity comes from the square pyramidal geometry of the metallacyclopentadiene intermediate **III** (Figure 1), ΔG = −29.8 kcal/mol, the molecular geometry of which is also supported by a previously obtained crystal structure.[57] The square pyramidal geometry of intermediate **III** positions one of the metallacyclopentadiene's phenyl substituents in the apical position, which is preferred over hydrogen in the apical position by 1.7 kcal/mol. This ultimately affects the insertion of the cyanamide moiety in the next step of the mechanism by leaving open a coordination site *trans* to the apical phenyl of the metallacyclopentadiene (Figure 4).

https://doi.org/10.1021/acscatal.1c03871
ACS Catal. 2021, 11, 14677−14687

A cyanamide will then coordinate to this site through the terminal nitrogen, resulting in intermediate **IV** (ΔG = −21.6 kcal/mol, Figure 1). Steric congestion prevents η^2-coordination of an alkyne to complex **III**.

Ligand Dissociation. Following η^1-coordination of cyanamide, the steric congestion in the ligand field is resolved by dissociation of one aldimine "arm" of the PDAI ligand from the Fe-center (intermediate **V**, ΔG = −20.1 kcal/mol, Figure 1). The dissociation of the ligand arm is critical in the reaction; a transition state wherein the cyanamide reacts with the metallacyclopentadiene without prior ligand arm dissociation was found to have an uncompetitively high energy barrier ($\Delta\Delta G^{\ddagger} \geq 23$ kcal/mol).

Experimental verification for ligand arm dissociation stems from the work performed by Chirik *et al.*, wherein it was previously shown that ligand arms on Fe-PDAI complexes are more labile than the analogue Fe-PDI complexes. The more rigid ligand framework impacts the overall catalyst stability by reducing open coordination sites on the Fe-center, which, in turn, has a significant potential impact on catalytic transformations.[91−94] In fact, we observe that Fe-PDI catalysts show differing reactivity, generating benzenes in low yield, while reactions conducted with Fe-PDAI yield pyridine product (Table 2, entries 1 and 2 versus entries 3 and 4, respectively).

Table 2. Evaluation of Ligand Framework-Dependent Reactivity in Intermolecular [2+2+2] Cycloaddition Reaction (Fe-PDAI Versus Fe-PDI Versus Fe-Hybrid)

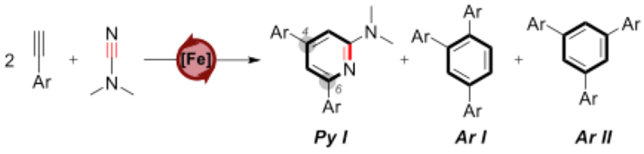

Entry	Ligand	Ar	Ratio[a] Py I : Ar I : Ar II	Yield[a] [%] Py I : Ar I : Ar II
1	^{Mes}PDAI	*p*-H	1.0 : 0.3 : 0.2	47 : 14 : 10
2	^{Mes}PDAI	*p*-Me	1.0 : 0.2 : 0.1	60 : 9 : 4
3	^{Mes}PDI	*p*-H	1.0 : 35 : 1.0	<1 : 13 : <1
4	^{Mes}PDI	*p*-Me	1.0 : 17 : 0.8	<1 : 6 : <1
5	^{Mes}Hybrid	*p*-H	1.0 : 0.6 : 0.1	22 : 13 : 3
6	^{Mes}Hybrid	*p*-Me	1.0 : 0.3 : 0.04	28 : 9 : <1

[Fe]: 10 mol% [(*Ligand*)$FeBr_2$], 10 mol% Zn, 25 mol% internal standard, THF 0.4 M, rt, 24h, *glovebox*.

[a] *GC Ratio's are based on Naphthalene as internal standard. The obtained yields are an average of two runs.*

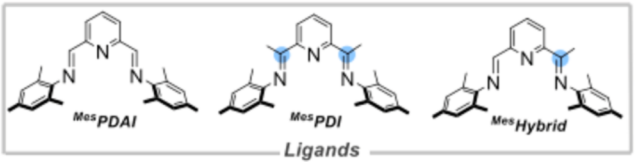

The observation of differences in ligand activity can be attributed to the computationally suggested ligand arm dissociation, which is more favorable for the PDAI ligand species. The dissociation of a ligand arm results in a rotation around the C_{pyr}−C_{imine} bond of the catalyst, allowing the η^1-coordinated cyanamide substrate to reach a reactive conformation with respect to the metallacyclopentadiene. Steric occlusion by a substituent other than hydrogen, e.g., methyl for PDI, on the imine carbon is hypothesized to prevent the cyanamide from reaching such a reactive conformation, explaining why the sterically congested Fe-PDI catalyst does not yield any 2-aminopyridine product. This hypothesis was further probed by applying a hybrid ligand bearing a ketimine as well as an aldimine arm in the [2+2+2] cycloaddition protocol; comparing the reaction results, we can observe a trend in the reactivity profile between these different Fe-catalysts. The reaction catalyzed by the [(^{Mes}PDAI)Fe(II)Br_2] complex (Table 2, entries 1 and 2) showed the highest yield of 4,6-disubstituted-2-aminopyridine, whereas the [(^{Mes}Hybrid)Fe(II)Br_2] complex (Table 2, entries 5 and 6) gave a lower conversion to 2-aminopyridine product, and the [(^{Mes}PDI)Fe(II)Br_2] complex (Table 2, entries 3 and 4) only gave trace pyridine product when used as catalytic species. The results of these test reactions are in good agreement with computational analysis and suggest that the degree of ligand arm lability has a crucial impact on the mechanism of this reaction.

Despite the agreement with our theory, we are well aware of a number of limitations to conclusively confirm our proposed ligand effects; for example, an important effect on catalytic performance could originate from the *in situ* reduction of the different catalyst species. It is shown in the literature that small changes on the PDAI/PDI framework result in drastic changes in synthetic protocols such as the efficiency of reducing agents.[91] Attempts to isolate stable Fe^0 complexes were unsuccessful in this study, and these effects are under investigation in the Louie laboratory to better understand the rate differential in all product distributions across the ligand set.

Insertion and Reductive Elimination. *Cyanamide Insertion.* Literature reports a variety of reaction pathways for [2+2+2] cycloaddition reactions based on Co,[76−79] Ru,[18,20,77,82] and Rh[77,80] catalysts.[1,6−8] Following cyanamide coordination and subsequent ligand arm dissociation, we explored several of these potential reaction pathways that could lead to the observed pyridine product. The first pathway was a [4+2] cycloaddition. In our hands, no concerted transition state could be located leading to the pyridine product; however, stepwise transition states were located with uncompetitively high barriers ($\Delta\Delta G$ > 30 kcal/mol).

We next considered a migratory insertion pathway, wherein the cyanamide would insert into one of the Fe-C bonds, leading directly to a 7-membered metallacycle. In our hands, no transition state leading directly to a 7-membered metallacycle could be found.[98] Instead, we discovered that a formal [2+2] cycloaddition process (**TS VI**, $\Delta G^{\ddagger}$ = −19.0 kcal/mol) was operative. This [2+2] process, while superficially reminiscent to that observed in olefin metathesis and Ru-catalyzed [2+2+2] processes, is instead more closely related to those observed in Ir-catalyzed [2+2+2] processes in that no double bond character is observed between the Fe-center and the hydrogen-bearing carbon of the metallacyclopentadiene in intermediate **V**.[81,82,95−97,99,100] Transition state **TS VI** thus led to bicyclic metallacyclobutene intermediate **VII**, ΔG = −39.5 kcal/mol.

https://doi.org/10.1021/acscatal.1c03871
ACS Catal. 2021, 11, 14677−14687

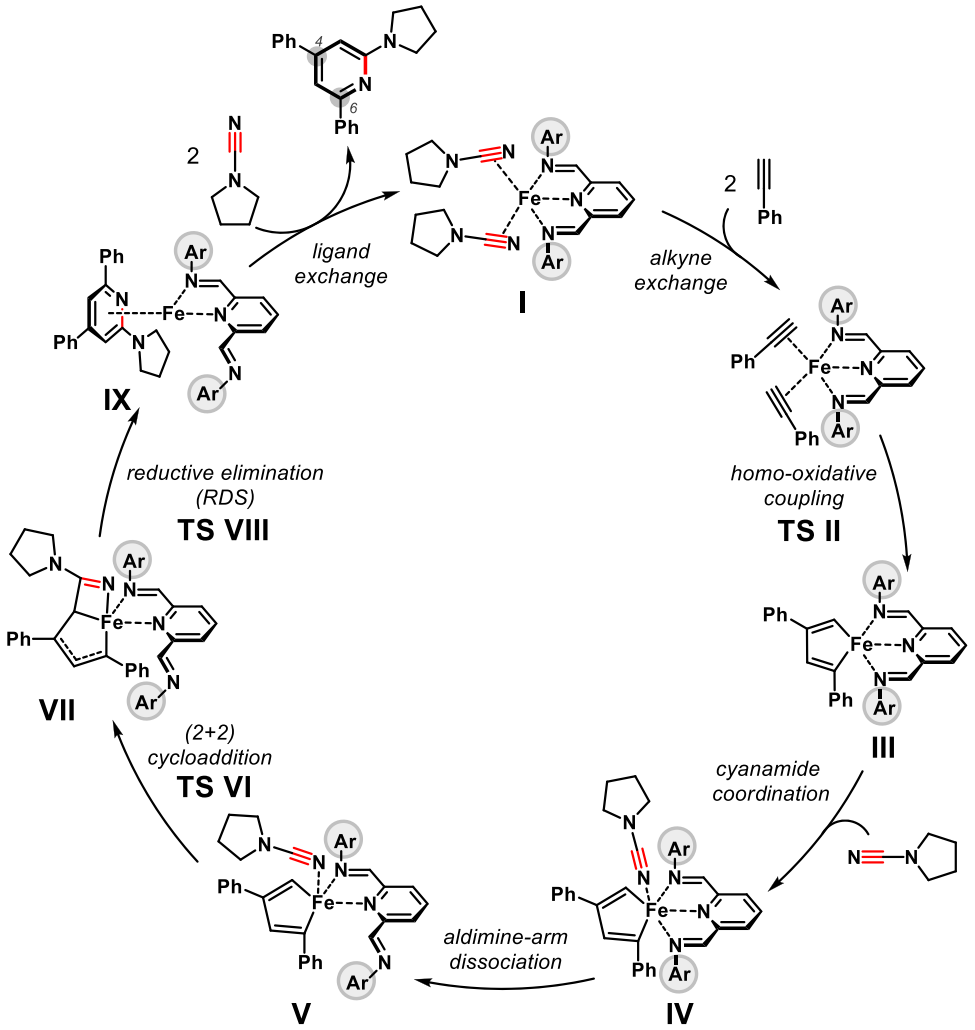

Figure 5. Proposed catalytic cycle.

Reductive Elimination. There are two possible pathways proceeding from intermediate **VII** to the product−catalyst complex. The first is a direct reductive elimination of the intermediate to form the product−catalyst complex (**TS-VIII**, $\Delta G^{\ddagger}$ = −25.2 kcal/mol; product−catalyst complex **IX**, ΔG = −68.5 kcal/mol).

The second pathway involves an electrocyclic ring opening of intermediate **VII** to form a 7-membered metallacycle. This 7-membered metallacycle would then undergo reductive elimination to yield the product−catalyst complex **IX**. Electrocyclic ring opening to the 7-membered ring was found to have a similar energetic barrier to direct reductive elimination ($\Delta G^{\ddagger}$ = −25.1 kcal/mol). However, reductive elimination from the 7-membered metallacycle (ΔG = −56.2 kcal/mol) was found to be slower overall than direct reductive elimination from intermediate **VII** ($\Delta G^{\ddagger}$ = −33.6 kcal/mol).

Thus, while both reductive elimination pathways are viable, formation of the product−catalyst complex **IX** directly from intermediate **VII** is a faster process than the formation of, and reductive elimination from, a 7-membered metallacycle (see the Supporting Information for further discussion).

Product/Substrate Exchange. Various coordination states of the pyridine ring to the PDAI catalyst were also computed, with the η^6-coordination state preferred by at least 0.6 kcal/mol. The barrier to catalyst turnover is −33.1 kcal/mol, indicating that there is no product−catalyst inhibition and resulting in facile re-coordination of cyanamide to the active catalytic species.

CONCLUSIONS

A detailed experimental and computational investigation into the origin of the observed chemo- and regioselectivities of the Fe-PDAI-catalyzed [2+2+2] cycloaddition reaction of alkynes and cyanamides to yield 2-aminopyridines has been conducted. Oxidative couplings, analogous to those proposed in Co- and Rh-catalyzed alkyne trimerization reactions,[20,76,77,82,99] are uniquely combined with the [2+2] cycloaddition reactions seen in Ru- and Ir-catalyzed processes. This combination is made possible by the lability of the PDAI ligand, and both of these steps play crucial roles in determining the chemo- and regioselectivity of the trisubstituted pyridine product (Figure 5).

A special interest is also focused on the expansion and generation of new chemical space—synthetic methodology where valuable heteroaromatic core structures like pyridines, aminopyridines, pyridones, and pyrimidines are easily accessible. The prevalence of these structural motifs in medicinal chemistry highlights the importance of endeavors such as the investigations conducted in this work.

https://doi.org/10.1021/acscatal.1c03871
ACS Catal. 2021, 11, 14677−14687

■ ASSOCIATED CONTENT

Supporting Information

The Supporting Information is available free of charge at https://pubs.acs.org/doi/10.1021/acscatal.1c03871.

Computed structures, energies, and thermal corrections (PDF)

General experimental; general synthesis pathway; general experimental details for competition experiment, Figures S1−S3 (PDF)

■ AUTHOR INFORMATION

Corresponding Authors

Paul H.-Y. Cheong − *Department of Chemistry, Oregon State University, Corvallis, Oregon 97331, United States;* orcid.org/0000-0001-6705-2962; Email: cheongh@oregonstate.edu

Janis Louie − *Department of Chemistry, The University of Utah, Salt Lake City, Utah 84112, United States;* orcid.org/0000-0003-3569-1967; Email: louie@chem.utah.edu

Authors

Jordan L. Harper − *Department of Chemistry, Oregon State University, Corvallis, Oregon 97331, United States;* orcid.org/0000-0002-5077-4050

Stephanie Felten − *Department of Chemistry, The University of Utah, Salt Lake City, Utah 84112, United States;* Present Address: Process Research & Development, MRL, Merck & Co. Inc., 126 E Lincoln Avenue, Rahway, New Jersey 07065, United States; orcid.org/0000-0002-5477-5026

Ryan M. Stolley − *Department of Chemistry, The University of Utah, Salt Lake City, Utah 84112, United States*

Alexander S. Hegg − *Department of Chemistry, The University of Utah, Salt Lake City, Utah 84112, United States;* Present Address: Department of Chemistry, Yale University, 225 Prospect Street, New Haven, Connecticut 06511, United States.

Complete contact information is available at: https://pubs.acs.org/10.1021/acscatal.1c03871

Author Contributions

[§]J.L.H. and S.F. contributed equally to this work.

Notes

The authors declare no competing financial interest.

■ ACKNOWLEDGMENTS

P.H.-Y.C. is the Bert and Emelyn Christensen professor of OSU, and gratefully acknowledges financial support from the Vicki & Patrick F. Stone family and the National Science Foundation (NSF, CHE-1352663). NMR experiments included in this publication were recorded at the David M. Grant NMR Center, a University of Utah Core Facility. Funds for the construction of the center and the helium recovery system were obtained from the University of Utah and the National Institutes of Health Awards 1C06RR017539-01A1 and 3R01GM063540-17W1, respectively. NMR instruments were purchased with the support of the University of Utah and the National Institutes of Health Award 1S10OD25241-01. Support for A. S. Hegg was provided by NSF REU grant 1659579.

■ ABBREVIATIONS

PDAI, pyridine dialdimine; PDI, pyridine diimide; TS, transition state; Mes, mesityl

■ REFERENCES

(1) Chopade, P. R.; Louie, J. [2+2+2] Cycloaddition Reactions Catalyzed by Transition Metal Complexes. *Adv. Synth. Catal.* **2006**, *348*, 2307−2327.

(2) Domínguez, G.; Perez-Castells, J. Recent advances in [2+2+2] cycloaddition reactions. *Chem. Soc. Rev.* **2011**, *40*, 3430−3444.

(3) Galan, B. R.; Rovis, T. Beyond Reppe: building substituted arenes by [2+2+2] cycloadditions of alkynes. *Angew. Chem., Int. Ed.* **2009**, *48*, 2830−2834.

(4) Gandon, V.; Aubert, C.; Malacria, M. Recent progress in cobalt-mediated [2 + 2 + 2] cycloaddition reactions. *Chem. Commun.* **2006**, 2209−2217.

(5) Heller, B.; Hapke, M. The fascinating construction of pyridine ring systems by transition metal-catalysed [2 + 2 + 2] cycloaddition reactions. *Chem. Soc. Rev.* **2007**, *36*, 1085−1094.

(6) Ruijter, E.; Broere, D. Recent Advances in Transition-Metal-Catalyzed [2+2+2]-Cyclo(co)trimerization Reactions. *Synthesis* **2012**, *44*, 2639−2672.

(7) Shaaban, M. R.; El-Sayed, R.; Elwahy, A. H. M. Construction of fused heterocycles by metal-mediated [2+2+2] cyclotrimerization of alkynes and/or nitriles. *Tetrahedron* **2011**, *67*, 6095−6130.

(8) Varela, J. A.; Saá, C. Construction of Pyridine Rings by Metal-Mediated [2 + 2 + 2] Cycloaddition. *Chem. Rev.* **2003**, *103*, 3787−3801.

(9) Cioni, P.; Diversi, P.; Giovanni, I.; Lucherin, A.; Ronca, P. Rhodium-Catalyzed Synthesis of Pyridines from Alkynes and Nitriles. *J. Mol. Catal.* **1987**, *40*, 331−357.

(10) Komine, Y.; Tanaka, K. Rhodium-Catalyzed Complete Regioselective Intermolecular Cross-Cyclotrimerization of Aryl Ethynyl Ethers and Nitriles or Isocyanates at Room Temperature. *Org. Lett.* **2010**, *12*, 1312−1315.

(11) Oberg, K. M.; Lee, E. E.; Rovis, T. Regioselective rhodium-catalyzed intermolecular [2+2+2] cycloaddition of alkynes and isocyanates to form pyridones. *Tetrahedron* **2009**, *65*, 5056−5061.

(12) Tanaka, K.; Hara, H.; Nishida, G.; Hirano, M. Synthesis of Perfluoroalkylated Benzenes and Pyridines through Cationic Rh(I)/Modified BINAP-Catalyzed Chemo- and Regioselective [2 + 2 + 2] Cycloaddition. *Org. Lett.* **2007**, *9*, 1907−1910.

(13) Tanaka, K.; Suzuki, N.; Nishida, G. Cationic Rhodium(I)/Modified-BINAP Catalyzed [2+2+2] Cycloaddition of Alkynes with Nitriles. *Eur. J. Org. Chem.* **2006**, *2006*, 3917−3922.

(14) Tanaka, K.; Takahashi, Y.; Suda, T.; Hirano, M. Synthesis of Enantioenriched N-Aryl-2-pyridones with Chiral C-N Axes by Rhodium-Catalyzed [2+2+2] Cycloaddition of Alkynes with Isocyanates. *Synlett* **2008**, *2008*, 1724−1728.

(15) Wada, A.; Noguchi, K.; Hirano, M.; Tanaka, K. Enantioselective Synthesis of C2-Symmetric Spirobipyridine Ligands through Cationic Rh(I)/Modified-BINAPCatalyzed Double [2 + 2 + 2] Cycloaddition. *Org. Lett.* **2007**, *9*, 1295−1298.

(16) Medina, S.; Domínguez, G.; Pérez-Castells, J. Efficient Generation of Pyridines by Ruthenium Carbene Mediated [2+ 2 + 2] Cyclotrimerization. *Org. Lett.* **2012**, *14*, 4982−4985.

(17) Trost, B. M.; Gutierrez, A. C. Ruthenium-Catalyzed Cycloisomerization-6pi-Cyclization: A Novel Route to Pyridines. *Org. Lett.* **2007**, *9*, 1473−1476.

(18) Xu, F.; Wang, C.; Li, X.; Wan, B. Ruthenium-catalyzed [2+2+2] cycloaddition of diynes with nitriles in pure water. *ChemSusChem* **2012**, *5*, 854−857.

(19) Yamamoto, Y.; Kinpara, K.; Ogawa, R.; Nishiyama, H.; Itoh, K. Ruthenium-catalyzed cycloaddition of 1,6-diynes and nitriles under mild conditions: role of the coordinating group of nitriles. *Chem. - Eur. J.* **2006**, *12*, 5618−5631.

(20) Yamamoto, Y.; Kinpara, K.; Saigoku, T.; Takagishi, H.; Okuda, S.; Nishiyama, H.; Itoh, K. Cp*RuCl-Catalyzed [2 + 2 + 2]

Cycloadditions of α,ω-Diynes with Electron-Deficient Carbon-Heteroatom Multiple Bonds Leading to Heterocycles. *J. Am. Chem. Soc.* **2005**, *127*, 605−613.
(21) Yamamoto, Y.; Ogawa, R.; Itoh, K. Significant Chemo- and Regioselectivies in the Ru(II)-Catalyzed [2 + 2 + 2] Cycloaddition of 1,6-Diynes with Dicyanides. *J. Am. Chem. Soc.* **2001**, *123*, 6189−6190.
(22) Yamamoto, Y.; Okuda, S.; Itoh, K. Ruthenium(ii)-catalyzed [2 + 2 + 2] cycloaddition of 1,6-diynes with electron-deficient nitriles. *Chem. Commun.* **2001**, 1102−1103.
(23) Yamamoto, Y.; Takagishi, H.; Itoh, K. Ruthenium(II)-Catalyzed Cycloaddition of 1,6-Diynes with Isocyanates Leading to Bicyclic Pyridones. *Org. Lett.* **2001**, *3*, 2117−2119.
(24) Zou, Y.; Liu, Q.; Deiters, A. Synthesis of the Pyridine Core of Cyclothiazomycin. *Org. Lett.* **2011**, *13*, 4352−4355.
(25) Hashimoto, T.; Ishii, S.; Yano, R.; Miura, H.; Sakata, K.; Takeuchi, R. Iridium-Catalyzed [2+2+2] Cycloaddition of α,ω-Diynes with Cyanamides. *Adv. Synth. Catal.* **2015**, *357*, 3901−3916.
(26) Hashimoto, T.; Kato, K.; Yano, R.; Natori, T.; Miura, H.; Takeuchi, R. Iridium-Catalyzed Synthesis of Acylpyridines by [2 + 2 + 2] Cycloaddition of Diynes with Acyl Cyanides. *J. Org. Chem.* **2016**, *81*, 5393−5400.
(27) Onodera, G.; Shimizu, Y.; Kimura, J. N.; Kobayashi, J.; Ebihara, Y.; Kondo, K.; Sakata, K.; Takeuchi, R. Iridium-catalyzed [2 + 2 + 2] cycloaddition of alpha,omega-diynes with nitriles. *J. Am. Chem. Soc.* **2012**, *134*, 10515−10531.
(28) Onodera, G.; Suto, M.; Takeuchi, R. Iridium-catalyzed [2+2+2] cycloaddition of alpha,omega-diynes with isocyanates. *J. Org. Chem.* **2012**, *77*, 908−920.
(29) Takeuchi, R.; Fujisawa, S.; Yoshida, Y.; Sagano, J.; Hashimoto, T.; Matsunami, A. Synthesis of Multisubstituted Azatriphenylenes by Iridium-Catalyzed [2 + 2 + 2] Cycloaddition of Biaryl-Linked Diynes with Nitriles. *J. Org. Chem.* **2018**, *83*, 1852−1860.
(30) Boñaga, L. V.; Zhang, H. C.; Maryanoff, B. E. Cobalt-mediated cyclotrimerisation of bis-alkynes and cyanamides. *Chem. Commun.* **2004**, *21*, 2394−2395.
(31) Boñaga, L. V. R.; Zhang, H.-C.; Moretto, A. F.; Ye, H.; Gauthier, D. A.; Li, J.; Leo, G. C.; Maryanoff, B. E. Synthesis of Macrocycles via Cobalt-Mediated [2 + 2 + 2] Cycloadditions. *J. Am. Chem. Soc.* **2005**, *127*, 3473−3485.
(32) Garcia, P.; Evanno, Y.; George, P.; Sevrin, M.; Ricci, G.; Malacria, M.; Aubert, C.; Gandon, V. Synthesis of aminopyridines and aminopyridones by cobalt-catalyzed [2+2+2] cycloadditions involving yne-ynamides: scope, limitations, and mechanistic insights. *Chem. - Eur. J.* **2012**, *18*, 4337−4344.
(33) Gray, B. L.; Wang, X.; Brown, W. C.; Kuai, L.; Schreiber, S. L. Diversity Synthesis of Complex Pyridines Yields a Probe of a Neurotrophic Signaling Pathway. *Org. Lett.* **2008**, *10*, 2621−2624.
(34) Groth, U.; Huhn, T.; Kesenheimer, C.; Kalogerakis, A. Cobalt-Mediated Regioselective Synthesis of Substituted Tetrahydroquinolines. *Synlett* **2005**, *11*, 1758−1760.
(35) (a) Heller, B.; Oehme, G. First Cobalt(i)-catalysed Hetero-cyclotrimerization of Ethyne with Nitriles to Pyridines in Water under Mild Conditions. *J. Chem. Soc., Chem. Commun.* **1995**, 179−180. (b) Wang, C.-S.; Sun, Q.; Garcia, F.; Wang, C.; Yoshikai, N. Robust Cobalt Catalyst for Nitrile/Alkyne [2+2+2] Cycloaddition: Synthesis of Polyarylpyridines and Their Mechanochemical Cyclodehydrogenation to Nitrogen-Containing Polyaromatics. *Angew. Chem., Int. Ed.* **2021**, *60*, 9627−9634.
(36) (a) Kase, K.; Goswami, A.; Ohtaki, K.; Tanabe, E.; Saino, N.; Okamoto, S. On-Demand Generation of an Efficient Catalyst for Pyridine Formation from Unactivated Nitriles and α,ω-Diynes Using CoCl2-6H2O, dppe, and Zn. *Org. Lett.* **2007**, *9*, 931−934. (b) Li, K.; Wei, L.; Sun, M.; Li, B.; Liu, M.; Li, C. Enantioselective Synthesis of Pyridines with All-Carbon Quaternary Carbon Centers via Cobalt-Catalyzed Desymmetric [2+2+2] Cycloaddition. *Angew. Chem., Int. Ed.* **2021**, *60*, 20204−20209.
(37) Senaiar, R. S.; Young, D. D.; Deiters, A. Pyridines via solid-supported [2 + 2 + 2] cyclotrimerization. *Chem. Commun.* **2006**, 1313−1315.
(38) Tanaka, K.; Hara, H.; Nishida, G.; Hirano, M. Synthesis of Perfluoroalkylated Benzenes and Pyridines through Cationic Rh(I)/Modified BINAP-Catalyzed Chemo- and Regioselective [2 + 2 + 2] Cycloaddition. *Org. Lett.* **2007**, *9*, 1907−1910.
(39) Yong, L.; Butenschon, H. The first cobalt catalyzed [2 + 2 + 2] alkyne cyclotrimerization in aqueous medium at room temperature. *Chem. Commun.* **2002**, 2852−2853.
(40) Zhou, Y.; Porco, J. A., Jr.; Snyder, J. K. Synthesis of 5,6,7,8-Tetrahydro-1,6-naphthyridines and Related Heterocycles by Cobalt-Catalyzed [2 + 2 + 2] Cyclizations. *Org. Lett.* **2007**, *9*, 393−396.
(41) Kumar, P.; Prescher, S.; Louie, J. A serendipitous discovery: nickel catalyst for the cycloaddition of diynes with unactivated nitriles. *Angew. Chem., Int. Ed.* **2011**, *50*, 10694−10698.
(42) Louie, J.; Zhong, Y.; Spahn, N.; Stolley, R.; Nguyen, M. 3,5-Disubstituted 2-Aminopyridines via Nickel-Catalyzed Cycloaddition of Terminal Alkynes and Cyanamides. *Synlett* **2015**, *26*, 307−312.
(43) McCormick, M. M.; Duong, H. A.; Zuo, G.; Louie, J. A Nickel-Catalyzed Route to Pyridines. *J. Am. Chem. Soc.* **2005**, *127*, 5030−5031.
(44) Stolley, R. M.; Duong, H. A.; Louie, J. Mechanistic Evaluation of the Ni(IPr)2-Catalyzed Cycloaddition of Alkynes and Nitriles to Afford Pyridines: Evidence for the Formation of a Key eta(1)-Ni(IPr)2(RCN) Intermediate. *Organometallics* **2013**, *32*, 4952−4960.
(45) Stolley, R. M.; Duong, H. A.; Thomas, D. R.; Louie, J. The discovery of [Ni(NHC)RCN]2 species and their role as cycloaddition catalysts for the formation of pyridines. *J. Am. Chem. Soc.* **2012**, *134*, 15154−15162.
(46) Stolley, R. M.; Maczka, M. T.; Louie, J. Nickel-Catalyzed [2+2+2] Cycloaddition of Diynes and Cyanamides. *Eur. J. Org. Chem.* **2011**, *2011*, 3815−3824.
(47) Tekavec, T. N.; Zuo, G.; Simon, K.; Louie, J. An in Situ Approach for Nickel-Catalyzed Cycloaddition. *J. Org. Chem.* **2006**, *71*, 5834−5836.
(48) Satoh, Y.; Obora, Y. Low-valent niobium-catalyzed intermolecular [2 + 2 + 2] cycloaddition of tert-butylacetylene and arylnitriles to form 2,3,6-trisubstituted pyridine derivatives. *J. Org. Chem.* **2013**, *78*, 7771−7776.
(49) Chen, Y. L.; Sharma, P.; Liu, R. S. Sulfonamide-directed gold-catalyzed [2+2+2]-cycloadditions of nitriles with two discrete ynamides to construct 2,4-diaminopyridine cores. *Chem. Commun.* **2016**, *52*, 3187−3190.
(50) Sheng, J.; Wang, Y.; Su, X.; He, R.; Chen, C. Copper-Catalyzed [2+2+2] Modular Synthesis of Multisubstituted Pyridines: Alkenylation of Nitriles with Vinyliodonium Salts. *Angew. Chem., Int. Ed.* **2017**, *56*, 4824−4828.
(51) D'Souza, B. R.; Lane, T. K.; Louie, J. Iron-Catalyzed Cycloaddition of Alkynenitriles and Alkynes. *Org. Lett.* **2011**, *13*, 2936−2939.
(52) Knoch, F.; Kremer, F.; Schmidt, U.; Zenneck, U.; et al. (η4-1,5-Cyclooctadiene)(η6-phosphinine)iron(0): Novel Room-Temperature Catalyst for Pyridine Formation. *Organometallics* **1996**, *15*, 2713−2719.
(53) Lane, T. K.; D'Souza, B. R.; Louie, J. Iron-catalyzed formation of 2-aminopyridines from diynes and cyanamides. *J. Org. Chem.* **2012**, *77*, 7555−7563.
(54) Lane, T. K.; Nguyen, M. H.; D'Souza, B. R.; Spahn, N. A.; Louie, J. The iron-catalyzed construction of 2-aminopyrimidines from alkynenitriles and cyanamides. *Chem. Commun.* **2013**, *49*, 7735−7737.
(55) Ramsay, W. On picoline and its derivatives. *London, Edinburgh Dublin Philos. Mag. J. Sci.* **1876**, *2*, 269−281.
(56) Richard, V.; Ipouck, M.; Merel, D. S.; Gaillard, S.; Whitby, R. J.; Witulski, B.; Renaud, J. L. Iron(II)-catalysed [2+2+2] cycloaddition for pyridine ring construction. *Chem. Commun.* **2014**, *50*, 593−595.
(57) Spahn, N. A.; Nguyen, M. H.; Renner, J.; Lane, T. K.; Louie, J. Regioselective Iron-Catalyzed [2 + 2 + 2] Cycloaddition Reaction Forming 4,6-Disubstituted 2-Aminopyridines from Terminal Alkynes and Cyanamides. *J. Org. Chem.* **2017**, *82*, 234−242.
(58) Wang, C.; Li, X.; Wu, F.; Wan, B. A simple and highly efficient iron catalyst for a [2+2+2] cycloaddition to form pyridines. *Angew. Chem., Int. Ed.* **2011**, *50*, 7162−7166.

https://doi.org/10.1021/acscatal.1c03871
ACS Catal. 2021, 11, 14677−14687

(59) Wang, C.; Wang, D.; Xu, F.; Pan, B.; Wan, B. Iron-catalyzed cycloaddition reaction of diynes and cyanamides at room temperature. *J. Org. Chem.* **2013**, *78*, 3065−3072.
(60) Eichberg, M. J.; Dorta, R. L.; Grotjahn, D. B.; Lamottke, K.; Schmidt, M.; Vollhardt, K. P. C. Approaches to the Synthesis of (+)-Strychnine via the Cobalt-Mediated [2 + 2 + 2] Cycloaddition: Rapid Assembly of a Classic Framework. *J. Am. Chem. Soc.* **2001**, *123*, 9324−9337.
(61) McIver, A.; Young, D. D.; Deiters, A. A General Approach to Triphenylenes and Azatriphenylenes: Total Synthesis of Dehydrotylophorine and Tylophorine. *Chem. Commun.* **2008**, *101*, 4750−4752.
(62) Parnell, C. A.; Peter, K.; Vollhardt, C. The Cobalt Way to Vitamin-B6 - Regioselective Construction of the Tetrasubstituted Pyridine Nucleus by Cobalt-Catalyzed Alkyne Nitrile Cooligomerizations. *Tetrahedron* **1985**, *41*, 5791−5796.
(63) Saá, C.; Critts, D. D.; Hsu, G.; Vollhardt, K. P. C. A Cobalt-Catalyzed Entrz into the Ergot Alkaloids: Total Synthesis of (+)-Lysergene and (+)-LSD. *Synlett* **1994**, *1994*, 487−489.
(64) Welsch, T.; Tran, H.-A.; Witulski, B. Total Syntheses of the Marine Illudalanes Alcyopterosin I, L, M, N, and C. *Org. Lett.* **2010**, *12*, 5644−5647.
(65) Yuan, C.; Chang, C.-T.; Axelrod, A.; Siegel, D. Synthesis of (+)-Complanadine A, an Inducer of Neurotrophic Factor Excretion. *J. Am. Chem. Soc.* **2010**, *132*, 5924−5925.
(66) Small, B. L.; Brookhart, M.; Bennett, A. M. Highly Active Iron and Cobalt Catalysts for the Polymerization of Ethylene. *J. Am. Chem. Soc.* **1998**, *120*, 4049−4050.
(67) Britovsek, G. J. P.; Gibson, V. C.; Kimberley, B. S.; Maddox, P. J.; Mastroianni, S.; McTavish, S. J.; Redshaw, C.; Solan, G. A.; Stro1mberg, S.; White, A. J. P.; Williams, D. J. Iron and Cobalt Ethylene Polymerization Catalysts Bearing 2,6-Bis(Imino)Pyridyl Ligands: Synthesis, Structures, and Polymerization Studies. *J. Am. Chem. Soc.* **1999**, *121*, 8728−8740.
(68) Chang, C. H.; Wu, Z. J.; Chiu, C. H.; Liang, Y. H.; Tsai, Y. S.; Liao, J. L.; Chi, Y.; Hsieh, H. Y.; Kuo, T. Y.; Lee, G. H.; Pan, H. A.; Chou, P. T.; Lin, J. S.; Tseng, M. R. A new class of sky-blue-emitting Ir(III) phosphors assembled using fluorine-free pyridyl pyrimidine cyclometalates: application toward high-performance sky-blue- and white-emitting OLEDs. *ACS Appl. Mater. Interfaces* **2013**, *5*, 7341−7351.
(69) Liu, M.; Su, S.-J.; Jung, M.-C.; Qi, Y.; Zhao, W.-M.; Kido, J. Hybrid Heterocycle-Containing Electron-Transport Materials Synthesized by Regioselective Suzuki Cross-Coupling Reactions for Highly Efficient Phosphorescent OLEDs with Unprecedented Low Operating Voltage. *Chem. Mater.* **2012**, *24*, 3817−3827.
(70) Wang, C.; Jung, G.-Y.; Batsanov, A. S.; Bryce, M. R.; Petty, M. C. New electron-transporting materials for light emitting diodes: 1,3,4-oxadiazole−pyridine and 1,3,4-oxadiazole−pyrimidine hybrids. *J. Mater. Chem.* **2002**, *12*, 173−180.
(71) Yamamoto, Y.; Ishii, J.-i.; Nishiyama, H.; Itoh, K. Ru(II)-Catalyzed Chemo- and Regioselective Cyclotrimerization of Three Unsymmetrical Alkynes through Boron Temporary Tether. One-Pot Four-Component Coupling via Cyclotrimerization/Suzuki-Miyaura Coupling. *J. Am. Chem. Soc.* **2004**, *126*, 3712−3713.
(72) Yamamoto, Y.; Ishii, J.-i.; Nishiyama, H.; Itoh, K. Cp*RuCl-Catalyzed Formal Intermolecular Cyclotrimerization of Three Unsymmetrical Alkynes through a Boron Temporary Tether: Regioselective Four-Component Coupling Synthesis of Phthalides. *J. Am. Chem. Soc.* **2005**, *127*, 9625−9631.
(73) Shintani, R.; Takano, R.; Nozaki, K. Rhodium-catalyzed asymmetric synthesis of silicon-stereogenic silicon-bridged arylpyridinones. *Chem. Sci.* **2016**, *7*, 1205−1211.
(74) Fatland, A. W.; Eaton, B. E. Cobalt-Catalyzed Alkyne−Nitrile Cyclotrimerization To Form Pyridines in Aqueous Solution. *Org. Lett.* **2000**, *2*, 3131−3133.
(75) Hilt, G.; Hengst, C.; Hess, W. Solvent-Dependent Regiochemical Cyclotrimerisation of Phenylacetylene with Cobalt Catalysts Containing Disulfide Ligands: A Case Study. *Eur. J. Org. Chem.* **2008**, *2008*, 2293−2297.
(76) Dahy, A. A.; Koga, N. Theoretical study of formation of pyridines by interaction of a cobaltacyclopentadiene with model nitriles (hydrogen cyanide or trifluoroacetonitrile): Electronic effects of nitriles on the reaction mechanism. *J. Organomet. Chem.* **2010**, *695*, 2240−2250.
(77) Dazinger, G.; Torres-Rodrigues, M.; Kirchner, K.; Calhorda, M. J.; Costa, P. J. Formation of pyridine from acetylenes and nitriles catalyzed by RuCpCl, CoCp, and RhCp derivatives—A computational mechanistic study. *J. Organomet. Chem.* **2006**, *691*, 4434−4445.
(78) Diercks, R.; Eaton, B. E.; Guertzgen, S.; Satish, J.; Matzger, A. J.; Radde, R. H.; Vollhardt, K. P. C. Cobalt-Catalyzed Cyclotrimerization of Alkynes: The Answer to the Puzzle of Parallel Reaction Pathways. *J. Am. Chem. Soc.* **1998**, *120*, 8860−8871.
(79) Hardesty, J. H.; Koerner, J. B.; Albright, T. A.; Lee, G.-Y. Theoretical Study of the Acetylene Trimerization with CpCo. *J. Am. Chem. Soc.* **1999**, *121*, 6055−6067.
(80) Orian, L.; van Stralen, J. N. P.; Bickelhaupt, F. M. Cyclotrimerization Reactions Catalyzed by Rhodium(I) Half-Sandwich Complexes: A Mechanistic Density Functional Study. *Organometallics* **2007**, *26*, 3816−3830.
(81) Yamamoto, Y.; Arakawa, T.; Ogawa, R.; Itoh, K. Ruthenium(II)-Catalyzed Selective Intramolecular [2 + 2 + 2] Alkyne Cyclotrimerizations. *J. Am. Chem. Soc.* **2003**, *125*, 12143−12160.
(82) Kirchner, K.; Calhorda, M. J.; Schmid, R.; Veiros, L. F. Mechanism for the Cyclotrimerization of Alkynes and Related Reactions Catalyzed by CpRuCl. *J. Am. Chem. Soc.* **2003**, *125*, 11721−11729.
(83) Sakata, K.; Shimada, S.; Takeuchi, R. Regioselectivity in the Iridium-Catalyzed [2 + 2 + 2] Cycloaddition of Unsymmetrical α,ω-Diynes with Nitrile: A DFT Study. *Organometallics* **2020**, *39*, 2091−2101.
(84) Wakatsuki, Y.; Nomura, O.; Kitaura, K.; Morokuma, K.; Yamazaki, H. On the Transformation of Bis(acetylene)cobalt to Cobaltacyclopentadiene. *J. Am. Chem. Soc.* **1983**, *105*, 1907−1912.
(85) Thakur, A.; Louie, J. Advances in nickel-catalyzed cycloaddition reactions to construct carbocycles and heterocycles. *Acc. Chem. Res.* **2015**, *48*, 2354−2365.
(86) Xu, X.; Goddard, W. A. The extended Perdew-Burke-Ernzerhof functional with improved accuracy for thermodynamic and electronic properties of molecular systems. *J. Chem. Phys.* **2004**, *121*, 4068−4082.
(87) Schuchardt, K. L.; Didier, B. T.; Elsethagen, T.; Sun, L.; Gurumoorthi, V.; Li, J.; Windus, T. L. Basis set exchange: A Community Database for Computational Sciences. *J. Chem. Inf. Model.* **2007**, *47*, 1045−1052.
(88) Frisch, M. J.; Trucks, G. W.; Schlegel, H. B.; Scuseria, G. E.; Robb, M. A.; Cheeseman, J. R.; Scalmani, G.; Barone, V.; Petersson, G. A.; Nakatsuji, H.; Li, X.; Caricato, M.; Marenich, A. V.; Bloino, J.; Janesko, B. G.; Gomperts, R.; Mennucci, B.; Hratchian, H. P.; Ortiz, J. V.; Izmaylov, A. F.; Sonnenberg, J. L.; Williams-Young, D.; Ding, F.; Lipparini, F.; Egidi, F.; Goings, J.; Peng, B.; Petrone, A.; Henderson, T.; Ranasinghe, D.; Zakrzewski, V. G.; Gao, J.; Rega, N.; Zheng, G.; Liang, W.; Hada, M.; Ehara, M.; Toyota, K.; Fukuda, R.; Hasegawa, J.; Ishida, M.; Nakajima, T.; Honda, Y.; Kitao, O.; Nakai, H.; Vreven, T.; Throssell, K.; Montgomery, J. A., Jr.; Peralta, J. E.; Ogliaro, F.; Bearpark, M. J.; Heyd, J. J.; Brothers, E. N.; Kudin, K. N.; Staroverov, V. N.; Keith, T. A.; Kobayashi, R.; Normand, J.; Raghavachari, K.; Rendell, A. P.; Burant, J. C.; Iyengar, S. S.; Tomasi, J.; Cossi, M.; Millam, J. M.; Klene, M.; Adamo, C.; Cammi, R.; Ochterski, J. W.; Martin, R. L.; Morokuma, K.; Farkas, O.; Foresman, J. B.; Fox, D. J. *Gaussian 09*, revision E.01; Gaussian, Inc.: Wallingford, CT, 2016.
(89) Gandon, V.; Agenet, N.; Vollhardt, P. C.; Malacria, M.; Aubert, C. Cobalt-Mediated Cyclic and Linear 2:1 Cooligimerization of Alkynes with Alkenes: A DFT Study. *J. Am. Chem. Soc.* **2006**, *128*, 8509−8520.
(90) Bickelhaupt, F. M.; Houk, K. N. Analyzing Reaction Rates with the Distortion/Interaction-Activation Strain Model. *Angew. Chem., Int. Ed.* **2017**, *56*, 10070−10086.
(91) Russell, S. K.; Milsmann, C.; Lobkovsky, E.; Weyhermuller, T.; Chirik, P. J. Synthesis, electronic structure, and catalytic activity of

https://doi.org/10.1021/acscatal.1c03871
ACS Catal. 2021, 11, 14677−14687

reduced bis(aldimino)pyridine iron compounds: experimental evidence for ligand participation. *Inorg. Chem.* **2011**, *50*, 3159−3169.
(92) Li, H.; Gonçalves, T. P.; Lupp, D.; Huang, K.-W. PN3(P)-Pincer Complexes: Cooperative Catalysis and Beyond. *ACS Catal.* **2019**, *9*, 1619−1629.
(93) Bart, S. C.; Lobkovsky, E.; Bill, E.; Wieghardt, K.; Chirik, P. J. Neutral-Ligand Complexes of Bis(imino)pyridine Iron: Synthesis, Structure, and Spectroscopy. *Inorg. Chem.* **2007**, *46*, 7055−7063.
(94) Joannou, M. V.; Hoyt, J. M.; Chirik, P. J. Investigations into the Mechanism of Inter- and Intramolecular Iron-Catalyzed [2 + 2] Cycloaddition of Alkenes. *J. Am. Chem. Soc.* **2020**, *142*, 5314−5330.
(95) Onodera, G.; Shimizu, Y.; Kimura, J.-N.; Kobayashi, J.; Ebihara, Y.; Kondo, K.; Sakata, K.; Takeuchi, R. Iridium-Catalyzed [2+2+2] Cycloaddition of α,ω-Diynes with Nitriles. *J. Am. Chem. Soc.* **2012**, *134*, 10515−10531.
(96) Paneque, M.; Poveda, M. L.; Rendón, N.; Mereiter, K. Reaction of the Iridacyclopentadiene TpMe2Ir(C(R)═C(R)C(R)═C(R))-(H2O) (R = CO2Me) with Alkynes. *Organometallics* **2009**, *28*, 172−180.
(97) Paneque, M.; Poveda, M. L.; Rendón, N.; Mereiter, K. Isolation of a Stable 1-Iridabicyclo[3.2.0]hepta-1,3,6-triene and Its Reversible Transformation into an Iridacycloheptatriene. *J. Am. Chem. Soc.* **2004**, *126*, 1610−1611.
(98) In our hands, transition states directly leading to a 7-membered metallacycle from the "arm-off" cyanamide-coordinated metallacyclopentadiene intermediate could not be located; such transition states are not stationary points along the reaction coordinate.
(99) (a) Grubbs, R. H.; Burk, P. L.; Carr, D. D. Consideration of the Mechanism of the Olefin Metathesis Reaction. *J. Am. Chem. Soc.* **1975**, *97*, 3265−3267. (b) Grubbs, R. H.; Carr, D. D.; Hoppin, C.; Burk, P. L. Consideration of the Mechanism of the Metal Catalyzed Olefin Metathesis Reaction. *J. Am. Chem. Soc.* **1976**, *98*, 3478−3483. (c) Herisson, J. L.; Chauvin, Y. Catalysis of Olefin Transformations by Tungsten Complexes. II. Telomerization of Cyclic Olefins in the Presence of Acylic Olefins. *Makromol. Chem.* **1971**, *141*, 161−176.
(100) Ernst, C.; Walter, O.; Dinjus, E. Cp*Ru-allylcarbene Complexes by Nucleophilic Attack of Cyclic Cp*Ru-Dicarbenes. *J. Organomet. Chem.* **2001**, *627*, 249−254.

https://doi.org/10.1021/acscatal.1c03871
ACS Catal. 2021, 11, 14677−14687